Applied Catalysis B: Environmental 91 (2009) 123–134

Contents lists available at ScienceDirect

Applied Catalysis B: Environmental

journal homepage: www.elsevier.com/locate/apcatb

Promotional mechanism of tungstation on selective catalytic reduction of NO_x by methane over $In/WO_3/ZrO_2$

Guohua Jing [a,b], Junhua Li [a,*], Dong Yang [a], Jiming Hao [a]

[a] Department of Environmental Science and Engineering, Tsinghua University, Beijing 100084, China
[b] Department of Environmental Science and Engineering, Huaqiao University, Xiamen 361021, China

ARTICLE INFO

Article history:
Received 5 December 2008
Received in revised form 27 April 2009
Accepted 12 May 2009
Available online 20 May 2009

Keywords:
$DeNO_x$
Selective catalytic reduction
Methane
Indium
Tungstated zirconia
InO^+
$HCOO^-$

ABSTRACT

The catalytic performance and promotional mechanism of tungstation for selective catalytic reduction of NO by methane over In-loaded tungstated zirconia (In/WZr) were investigated. A clear improvement of catalytic activity was found over In/WZr catalysts. The highest NO conversion of 70% was achieved over a 1% In/WZr catalyst at 450 °C and 12,000 h^{-1}. In contrast, the maximum NO conversions of WZr, ZrO_2 and In/ZrO_2 were only 12%, 31% and 20%, achieved at 500, 650 and 600 °C, respectively. Tungstation was observed to influence the properties of catalysts in three aspects: (i) modify the existent state of surface indium species; (ii) determine the activation species of CH_4; (iii) cooperate with the loading of indium to enhance the formation and reduction of the intermediates. Differences in the existent state of indium and the activation species of CH_4 result in different catalytic activities and mechanisms for CH_4-SCR of NO. X-ray photoelectron spectroscopy measurements and Py-IR analysis showed that indium species on the In/ZrO_2 catalyst was in the In_2O_3 bulk phase due to the lack of Brønsted acid sites. However, the tungstated In/WZr catalyst possessed strong Brønsted acid sites, which was beneficial to the formation of active InO^+ species. DRIFTS studies further revealed the reaction intermediates of CH_4-SCR of NO on the tungstated and the untungstated catalysts. On In/ZrO_2 and ZrO_2, the activation species of CH_4 was the fully oxidized products CO_2 and H_2O. While on WZr and In/WZr, $HCOO^-$, the real reductant for CH_4-SCR of NO, was detected as the main intermediate species. In addition, the formation of $HCOO^-$ and the reduction of nitrate species were greatly accelerated by the synergistic effect between InO^+ and tungstation, which might explain the higher catalytic activity of In/WZr in comparison with WZr and In/ZrO_2.

1. Introduction

Methane is the most potential reductant for selective catalytic reduction (SCR) of NO_x due to its cheap cost and abundant availability [1,2]. Indium supported catalysts such as In/zeolite [3–12] and In/SZr (sulphated zirconia) [13] have been reported to be effective catalysts for CH_4-SCR. Among these catalysts, only a few catalysts, such as In, Co-FER, showed a good performance under hydrothermal conditions [10]. Tungstated zirconia (WZr) is more stable than zeolite and SZr support. More specifically, WZr possesses strong acid sites which are indispensable to the high activity and selectivity in CH_4-SCR [14]. Therefore, WZr might be a good choice for CH_4-SCR of NO_x. Chin et al. [13,15] reported that Pd supported on WZr showed a good performance for the CH_4-SCR reaction. WZr is able to stabilize the highly dispersed Pd^{2+} species (which are believed to be the active sites for catalytic reduction of NO with methane) in a similar manner as the acidic zeolites [16,17]. Recently, our group found that a catalyst of indium supported WZr showed high catalytic activity for the CH_4-SCR, even higher than that of Pd/WZr [18], which indicated that this catalyst might be more practicable in real exhaust condition. However, the influence of the tungstation and the promotional mechanism of CH_4-SCR over In/WZr have not been elucidated. In order to understand the information and the possible reaction pathways, the reaction surface intermediates and the nature of the active sites need to be identified.

Intrazeolite indium oxo species (InO^+) was commonly accepted as an active site of the CH_4-SCR process in many indium supported zeolite catalysts [5–7,19–21]. Our previous report [18] also suggested that InO^+ was the active site in NO reduction, but the role of the tungstation on the formation of the active site is still unclear. Regarding the reaction mechanism, many investigations have focused on the fundamental aspects of the reduction of NO catalyzed by metal-exchanged zeolites [6,22–29] and sulphated zirconia [30,31], but the catalysts with a different carrier or active

* Corresponding author. Tel.: +1 734 6473884/86 10 62782030; fax: +86 10 62785687.
E-mail address: lijunhua@tsinghua.edu.cn (J. Li).

0926-3373/$ – see front matter © 2009 Published by Elsevier B.V.
doi:10.1016/j.apcatb.2009.05.015

constituent experienced a distinguishing reaction mechanism. Lonyi et al. [24] claimed that NO^+ and NH_3 are commonly formed surface species that are conceivably the key reaction intermediates of NO-SCR with CH_4 over Co-, Co-, Pt-, and H-mordenite catalysts. According to the proposal of Maunula et al. [6], the adsorbed H_2NCO intermediate, formed in the reaction between NO_2 and partially oxidized methane, acts as an actual NO reductant in the reaction mechanism over In/ZSM-5 catalyst. Cowan et al. [25] and Satsuma et al. [26] have proposed that ammonia may be a possible intermediate in the reduction of NO with methane on Co/ZSM5. Shimizu et al. [27] detected the intermediate of NH_4^+ species on Pd-H-mordenite catalyst. The NH_4^+ species reacted with the nitrosyl species adsorbed on Pd^{2+} to produce N_2 and CO_2. However, Montanari et al. [28] proposed that the isocyanate (NCO) species, produced from the activation of CH_4 by the $Co^{3+}NO_3^-Co^{3+}$ species, is the active intermediate of CH_4-SCR. Over Pd-H-ZSM-5, the formation of surface nitrile (CN) species, formed from the decomposition of nitrosomethene (CH_2NO), was also suggested to precede the conversion of NO or NO_2 to N_2 [29]. In addition, mechanisms of CH_4-SCR on solid superacid catalysts have been reported recently. Kantcheva and Vakkasoglu [30,31] substantiated that HCOOH, formed from CH_4 activation on Co^{2+} sites, is a key intermediate to the conversion of NO_3^- to N_2 over the Co/SZr catalyst. While on the Pd/WZr catalyst, three intermediates, namely the CH_3NO_2, CH_3ONO and $HCOO^-$ species, were observed. However, only $HCOO^-$, produced by the decomposition of the nitromethane and cis-methyl nitrite isomers, acted as a reductant of the adsorbed NO producing nitrogen [32]. However, few studies on the mechanisms of CH_4-SCR have focused on tungstate zirconia, with the exception of Pd/WZr.

Considering the difference in the active center of In- and Pd-doped WZr catalysts, we herein report the promotional mechanism of tungstation on In-loaded tungstated zirconia for CH_4-SCR reactions. The acidity of the samples was studied by pyridine adsorption infrared analysis. The in situ DRIFTS method is applied to compare the formation, role, and activity of the surface-adsorbed species on the catalysts of WZr, In/ZrO_2 and In/WZr. Combining the results of catalytic activity and characterization studies, the relationship between tungstation and promotional mechanism is fully discussed, which might help to explain the significantly high activity of In/WZr as compared with that of WZr and In/ZrO_2 in the CH_4/NO-SCR reaction.

2. Experimental

2.1. Catalysts preparation

WZr, In/ZrO_2 and In/WZr catalysts were prepared by an impregnation method described in our earlier paper [18]. The tungstated zirconia (WZr) support was prepared by impregnating zirconium oxyhydroxide (AR grade, Shanghai Chemical Reagent Work, China) with an aqueous solution of ammonium paratungstate (AR grade, Tianjin Juneng Chemical Factory, China) and the W contents in the final supports were 10 wt.%. The supports were then dried at 120 °C overnight and calcined at 600 °C for 5 h. The zirconia support was obtained by directly calcinating zirconium oxyhydroxide at 600 °C for 5 h. Indium loading (1 wt.%) was accomplished by an impregnation method using an aqueous solution of indium nitrate (AR grade, Sinopharm Chemical Reagent Factory, China). After being dried at 110 °C overnight, the impregnated sample was then calcined in air at 650 °C for 5 h. The resulting catalysts are hereafter referred to as In/WZr and In/ZrO_2, where In refers to indium, and where WZr and ZrO_2 suggest that the supports used in these catalysts are WZr and ZrO_2, respectively. Ce modified catalyst CeIn/WZr was prepared by grinding CeO_2 together with In/WZr as described in our earlier paper [33]. The weight content of CeO_2 in catalysts was 10%. The BET surface area, pore size, and pore volume of the obtained CeO_2 were 38 m^2/g, 9.9 nm, and 0.39 cm^3/g, respectively.

2.2. Catalytic activity measurements

The activity measurements were carried out with a fixed-bed quartz reactor (i.d. 8 mm) in a temperature range of 300–600 °C. The feed gas was a mixture of 1000 ppm NO, 3000 ppm CH_4, 10% O_2, 0% or 10% H_2O and N_2 as the balance gas. The amount of catalyst was 0.25 g in every experiment and the space velocity was approximately 12,000 h^{-1}. NO and NO_2 concentration was analyzed with a chemiluminescence NO/NO_2 analyzer (Thermal Environmental Instruments, model 42C), and CH_4 concentration was measured by gas chromatograph (Shimadzu GC 17A). Catalyst activity was evaluated in the terms of percent of NO_x and CH_4 conversion, defined as:

$$\frac{C_{in} - C_{out}}{C_{in}} \times 100\%$$

where C_{in} and C_{out} are the NO_x and CH_4 concentrations at the reactor inlet and outlet, respectively. The activity data were collected after the catalytic reactions were substantially reached to the steady-state conditions for half an hour each temperature.

2.3. Py-IR analysis

Pyridine adsorption infrared spectrum measurements (Py-IR) characterization was performed in a MAGNA-IR 560 E.S.P model FTIR apparatus equipped with a smart collector and an MCT detector cooled by liquid N_2. The spectra were recorded at a resolution of 4 cm^{-1} and with a scan number of 64. The catalyst was finely ground and placed in a ceramic crucible. The catalyst was pretreated at vacuum condition (350 °C, 1×10^{-3} Pa) for 2 h and then cooled to room temperature, and then a spectrum of the catalyst was taken as the background. After adsorbing pyridine, the catalyst was temperature programmed to a setting point (200 or 350 °C) for vacuum treatment of 30 min (1×10^{-3} Pa). After cooled to room temperature, the IR spectrum of the catalyst was recorded from 1700 to 1400 cm^{-1}.

2.4. In situ DRIFTS studies

In situ DRIFTS spectra were recorded by a Nicolet NEXUS 870-FTIR spectrometer equipped with a smart collector and an MCT detector cooled by liquid N_2. The diffuse reflectance FT-IR measurements were carried out in situ in a high temperature cell, fitted with ZnSe windows. The catalyst was finely ground and placed in a ceramic crucible and manually pressed. Mass flow controllers and a sample temperature controller were used to simulate the real reaction conditions. Prior to each experiment, the catalyst was heated to 550 °C in 10% O_2/N_2 with a total flow rate of 100 mL/min for 30 min, and then cooled to the desired temperature. A spectrum of the catalyst in gas flow of 20 mL/min N_2 was taken as the background after dwelling for 20 min at a given temperature. The diluted reaction gases were introduced in the chamber and the final composition were about 1000 ppm NO, 10% O_2 and/or 3000 ppm CH_4 in N_2 (total flow rate 20 mL/min). If not specified, the sample spectra reported here were collected after dwelling for 20 min. The spectra were recorded at a resolution of 4 cm^{-1}. In order to clarify the surface phenomena and species occurring during the reaction process of CH_4/NO/SCR in the presence of oxygen, five different experiments were performed. (1) An "NO_x adsorption–desorption" experiment was designed to recognize the adsorbed nitrate species and their stability, which involved the formation of surface NO_x species by NO + O_2 coadsorption, followed by purging with N_2 flow at room temperature and then heating the closed IR cell containing the

NO_x precovered catalyst at the temperatures of 250, 300, 350 and 400 °C. (2) A "CH_4 activation" experiment was designed to confirm the active intermediate species of CH_4 activation, consisting of interaction of the pretreated catalyst with CH_4 at 250 and 350 °C. (3) A "NO_x-CH_4 reaction" experiment was designed to clarify the interaction of CH_4 with the catalyst containing adsorbed NO_x species at various temperatures. Stable NO_x species pre-adsorbed on the catalyst were formed in the same way as described in the NO_x adsorption experiment above. After taking the spectrum at 250 °C, methane was added to the gas flow and spectra were collected at the temperatures of 250, 300, 350 and 400 °C respectively. (4) A "steady-state reaction" experiment was performed to investigate the species formed during dynamic stable CH_4-SCR of NO_x at various temperatures, in other words, the spectrum was collected at the temperatures of 300, 350, 400, 450 and 500 °C with the continuous flowing of the inlet gas of NO, O_2 and CH_4. (5) A "transient reaction" experiment was performed to obtain information about the real-time change of the species on the working catalyst of In/WZr at 400 °C with sudden changing the component of the inlet gas. In one case, the pretreated catalyst first reacted with a gas mixture of CH_4 and O_2 for 15 min, and then NO was added to the gas flow. After another 15 min, CH_4 was removed from the gas mixture. In another case, NO and O_2 coadsorption was first performed, and then CH_4 was added to the gas mixture, and after 15 min, NO was removed from the gas flow. The real-time spectrum was collected during the entire process.

3. Results

3.1. Catalytic activities

Fig. 1(a) and (b) shows the NO_x and CH_4 conversion activities over WZr, In/WZr, In/ZrO_2 and ZrO_2 catalysts as a function of temperature, respectively. On ZrO_2, NO_x conversion increased with the increasing of temperature, and the maximum conversion efficiency was 31% at 650 °C. The loading of indium on ZrO_2 led to a pronounced decrease in NO_x conversion activity, but showed no influence on the activity for CH_4 conversion. The WZr showed significantly reduced activities for both NO_x and CH_4 conversion than that of the ZrO_2, the maximum NO_x conversion being only 12% at 500 °C. However, the presence of indium greatly enhanced the NO_x conversion of WZr, and the T_{max} (temperature for maximum NO conversion) was shifted to lower temperatures. The highest NO conversion rate for In/WZr catalyst reached 70% at 450 °C, and then decreased at higher temperature, due to the combustion of CH_4 by O_2.

The effect of NO_2 on NO_x conversion activity over In/WZr catalysts is shown in Fig. 2. As shown in Fig. 2, whether O_2 exists or not, the catalytic activity of In/WZr has been improved greatly by the substitution of NO with NO_2. The maximum NO_x conversion was increased from 14% (NO + CH_4) to 90% (NO_2 + CH_4) without O_2 and from 70% (NO + O_2 + CH_4) to 91% (NO_2 + O_2 + CH_4) with 10% O_2, respectively. The results indicated that NO_2 was more active than NO in CH_4-SCR process over In/WZr catalyst, which means the essence of CH_4-SCR might be the reaction between NO_2 and CH_4. That is to say, NO_2 is an important intermediate in CH_4-SCR reaction, while the function of O_2 is to induce the conversion of NO to NO_2. When the reaction gas is NO and CH_4, the experimental conditions did not approach the thermodynamic equilibrium due to no oxygen. When the reaction system with O_2, NO_2 will be generated then NO_x conversion increased. Moreover, it is difficult for the oxidation of NO to NO_2, and then the thermodynamic equilibrium needs more time than the SCR of NO_x with CH_4. Therefore, many researchers [8,34] think that the oxidation of NO to NO_2 is rate determine step in the CH_4-SCR. The addition of metal oxides (CeO_2, Al_2O_3, etc.) can greatly improve the catalytic activity

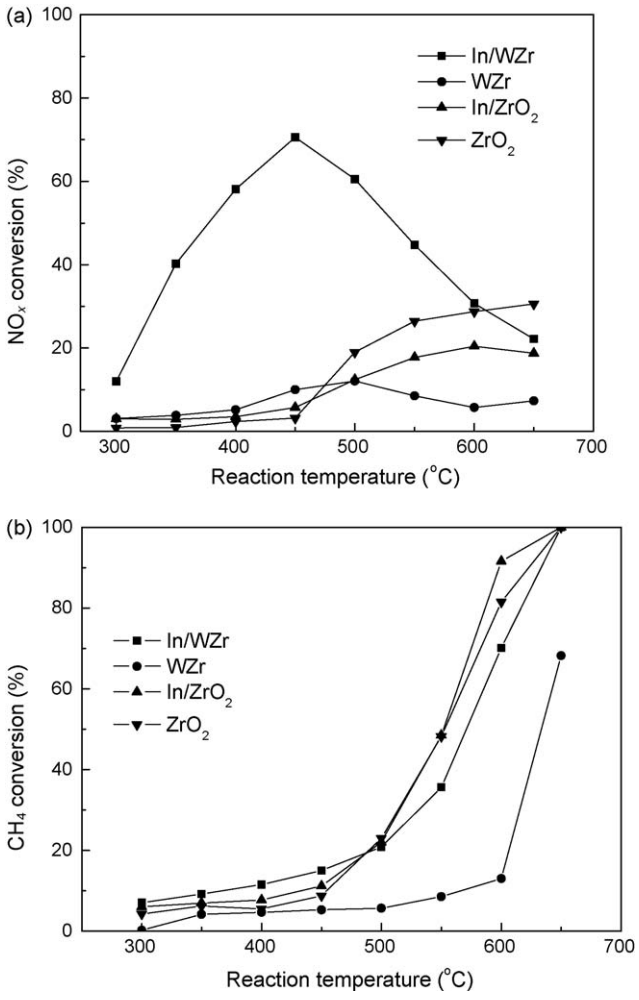

Fig. 1. NO_x and CH_4 conversions over ZrO_2, In/ZrO_2, WZr, and In/WZr [18]. (a) NO_x conversion; (b) CH_4 conversion. Reaction conditions: 1000 ppm NO, 3000 ppm CH_4, 10% O_2, N_2 as balance, GHSV = 12,000 h^{-1}.

by increasing the oxidation rate of NO to NO_2. As expected, the maximum NO_x conversion activity of the In/WZr catalyst was greatly improved from 40% to 92% with the increase of CeO_2 loading from 0% to 10% at a GHSV of 24,000 h^{-1} [33].

Influence of water vapor on the NO_x conversion activities of In/WZr, CeIn/WZr was shown in Fig. 3. The addition of 10% water

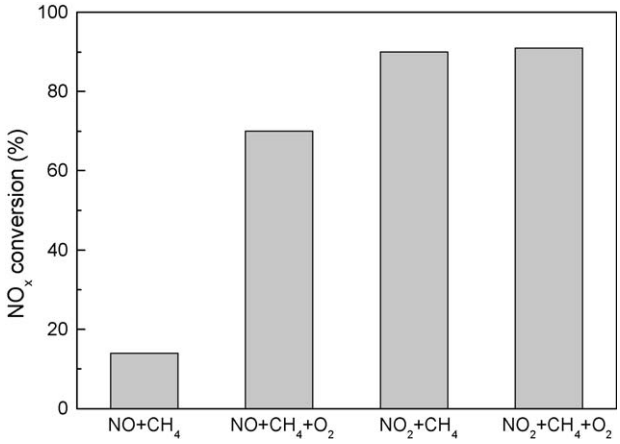

Fig. 2. Effect of NO_2 on NO_x conversion activity over In/WZr catalyst. Reaction conditions: 1000 ppm NO or NO_2, 3000 ppm CH_4, 0% or 10% O_2, N_2 as balance, GHSV = 12,000 h^{-1}.

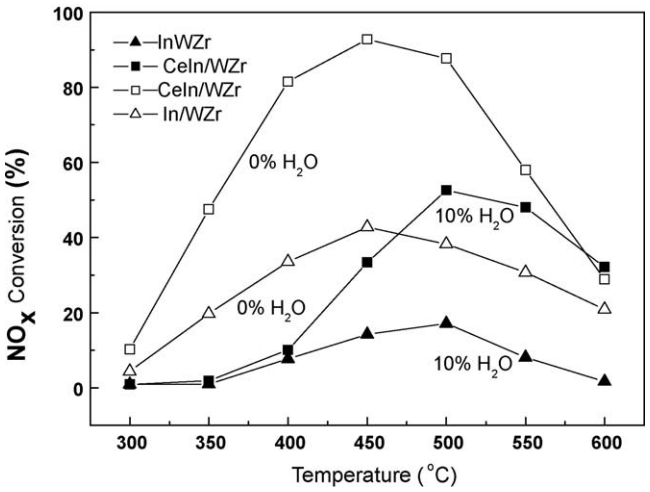

Fig. 3. The effect of H_2O on NO_x conversion activity over In/WZr and CeIn/WZr catalysts. Reaction conditions: 1000 ppm NO, 3000 ppm CH_4, 10% O_2, 0% or 10% H_2O, N_2 as balance, GHSV = 24,000 h^{-1}.

vapor to the feed gas reduced the catalytic activities of both of the two catalysts, and the T_{max} over the two catalysts all shifted from 450 to 500 °C. This deactivation was probably due to the adsorption of H_2O on InO^+ sites and forming inactive $In(OH)^{2+}$ species. The maximum NO_x conversion over the In/WZr decreased from 43% to 17%. While the maximum NO_x conversion on the CeIn/WZr catalyst could still reach 52% [33].

3.2. Characterization of catalysts

Fig. 4(a)–(c) presents the pyridine adsorption infrared spectra of WZr, In/WZr and ZrO_2 after vacuum treatment at 200 and 350 °C, respectively. Based on literatures [35,36], when pyridine is adsorbed on the Lewis and Brønsted acid sites of the catalysts, vibration peaks will emerge at 1450 and 1540 cm^{-1}, respectively. These two peaks distinguish the types (Brønsted or Lewis), relative amounts, and strength of the acids on the surface of catalysts. On WZr, from Fig. 4(a), we can see the peaks of Brønsted and Lewis acid appeared simultaneously and the peaks' strength presented a greater amount of Lewis acids sites than Brønsted sites at 200 °C. Increasing the temperature to 350 °C, the peaks of Lewis acids decreased sharply while the peaks of Brønsted acids changed only slightly. The result implied that, on WZr, the acid strength of the Lewis sites was weak, while that of Brønsted sites was strong. The results on In/WZr (Fig. 4(b)) were similar to that of WZr, indicating the loading of indium on WZr had no obvious effect on the acidity of the carrier. However, on ZrO_2, the results were the opposition. As shown in Fig. 4(c), the FT-IR spectra of ZrO_2 consisted only of bands of the Lewis acid–pyridine complex at about 1450 cm^{-1}. The intensities of such bands decreased with the evacuation temperatures. It is clear that the ZrO_2 possesses predominantly weak Lewis acid sites, which were similar to that reported in literature [37]. Therefore, the higher catalytic activity of In/WZr than In/ZrO_2 might be attributed to the existence of Brønsted acid sites on the tungstated carrier, which might also be responsible for the formation of the active center of InO^+. The relationship between the formation of InO^+ and the high catalytic activity of In/WZr with the effect of tungstation will be discussed later.

3.3. DRIFT studies

3.3.1. Nitrate species formed from NO_x adsorption–desorption

Infrared spectra of stable, adsorbed nitrate species formed from NO + O_2 mixture at room temperature (RT). The changes during

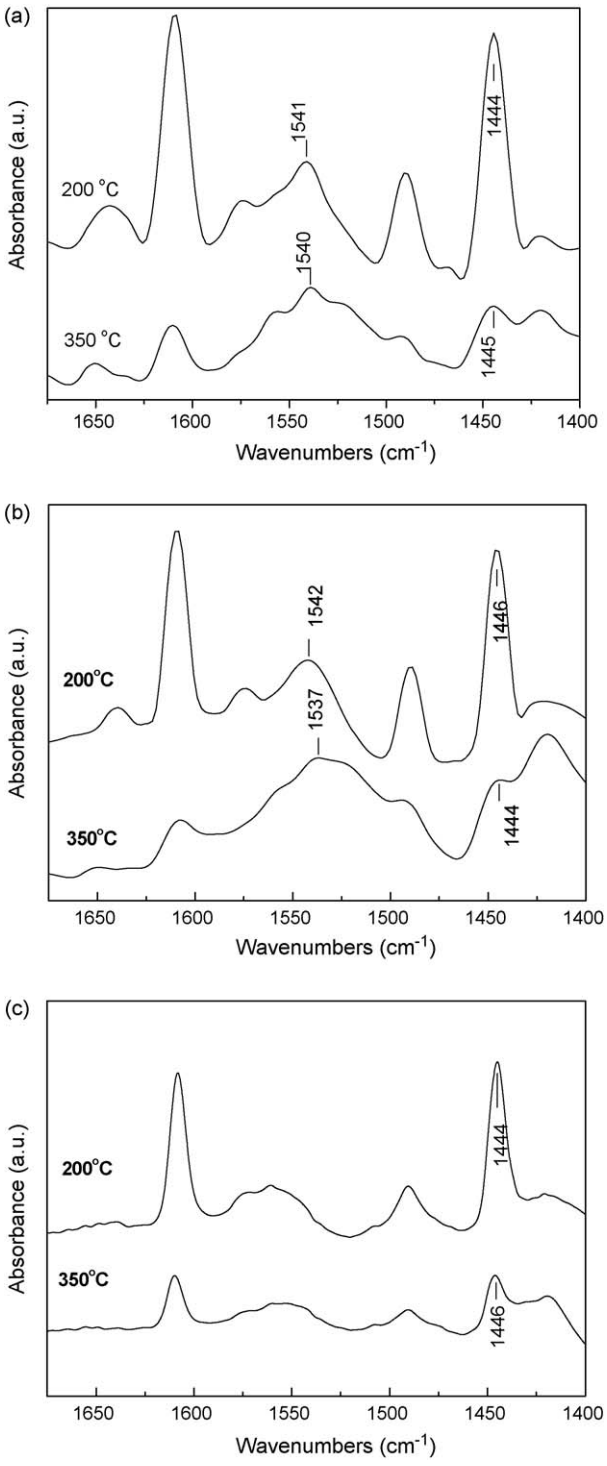

Fig. 4. Py-IR spectra of WZr (a), In/WZr (b) and ZrO_2 (c) after vacuum treatment at 200 and 350 °C.

high temperature desorption (250–400 °C) with the blowing of N_2 over In/ZrO_2, WZr and In/WZr are shown in Fig. 5(a)–(c), respectively. From the adsorption of NO + O_2 on In/ZrO_2 at room temperature (Fig. 5(a) spectrum RT), strong infrared absorption bands were obtained, identified as bands of bridging nitrate (1623 and 1013 cm^{-1}) and bidentate nitrate (1585 and 1034 cm^{-1}) groups [30,38,39]. The peak of 1236 cm^{-1} might be the overlap peaks of the bridging nitrate (1240 cm^{-1}) and the bidentate nitrate (1224 cm^{-1}). The peaks at 1516 and 1292 cm^{-1} are attributed to the monodentate nitrate due to the instability at high temperature.

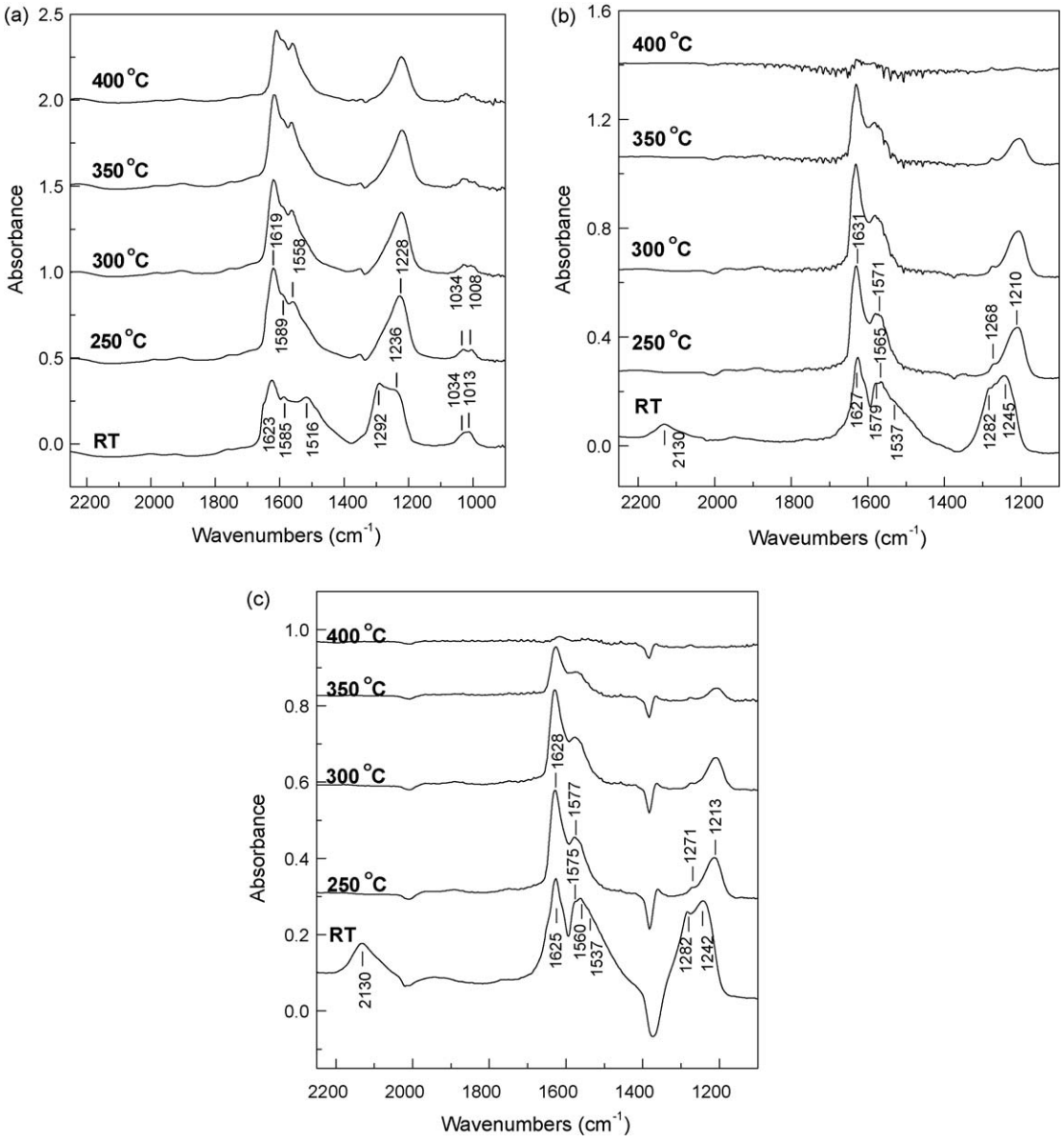

Fig. 5. In situ DRIFT spectra of surface nitrate species over In/ZrO_2 (a), WZr (b) and In/WZr (c) formed from NO + O_2 mixture at room temperature and their stability during high temperature thermal desorption in flowing gas of N_2 at 250, 300, 350 and 400 °C.

After the temperature arrived at 250 °C, the peaks at 1516 and 1292 cm^{-1} disappeared, while the intensity of the bands at 1619, 1589 and 1228 cm^{-1} obviously increased. Meanwhile, a new absorption band developed at about 1558 cm^{-1}, which might be another bidentate nitrate, different from the bidentate nitrate species vibration at 1589 cm^{-1}. These results strongly suggest that unstable monodentate nitrate converts to more stable bridging and bidentate nitrate at high temperatures. With continued temperature rise, the adsorbed nitrate species ceased changing types, but decreased in intensity. A large amount of nitrate species still exists steadily at a high temperature of 400 °C.

Regarding the catalysts of WZr and In/WZr, infrared absorption and desorption bands of nitrate species were completely congruent (Fig. 5(b) and (c)). The absorption in the 1650–1200 cm^{-1} region, detected on both samples at room temperature, are characteristic of various types of surface nitrate, identified as a bridging nitrate specie at 1627 cm^{-1} and two types of bidentate nitrate species at 1579 and 1565 cm^{-1} respectively. The peaks that disappeared at high temperature at 1537 and 1282 cm^{-1} were assigned to the unstable monodentate nitrate. The peak at 1245 cm^{-1} was the overlap of ν_{as} (NO_2) vibration of the bridging and bidentate nitrate species. While the peak at 2130 cm^{-1} stemmed from the ν_{NO} vibration of adsorbed NO^+ species, there are no special peaks of nitrate species belonging to InO^+ site here. According to the literatures [40,41], the peaks generated from the nitrate species adsorbed on InO^+ were at 1619 and 1557 cm^{-1}, which were overlapped by the peaks of the bridging and bidentate nitrate species adhering on the carrier of WZr. As a result, the former might be covered up by the latter, and fail to be detected in our tests. During desorption at 250 °C, the peak at 1537 cm^{-1} faded away while the peaks at 1282 cm^{-1} shifted to 1268 cm^{-1} and also decreased significantly in strength. On the contrary, the peaks attributed to bridging and bidentate nitrate species (1631 and 1571 cm^{-1}) were intensified, which indicated the conversion of monodentate nitrate to bridging and bidentate nitrate. With the further rising in temperature, the types of the adsorbed nitrate species ceased changing. The intensities decreased until the temperature arrived at 400 °C, at which all of the nitrate species disappeared, differing from the results on In/ZrO_2.

Table 1 summarizes the peak assignment of NO_x adspecies on In/ZrO_2, WZr and In/WZr based catalysts in NO + O_2 mixture.

Table 1
Assignment of the IR bands in NO_x adsorption and desorption experiments.

Catalyst	Species	Wave numbers (cm^{-1})	Vibration
In/ZrO_2	Bridging nitrate	1623–1619	ν(N═O)
	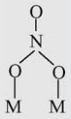	1240 1013	$\nu_{as}(NO_2)$ $\nu_s(NO_2)$
	Bidentate nitrate	1589–1585, 1558	ν(N═O)
	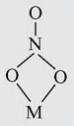	1224 1034	$\nu_{as}(NO_2)$ $\nu_s(NO_2)$
	Monodentate nitrate	1516	$\nu_{as}(NO_2)$
	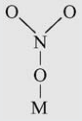	1292	$\nu_s(NO_2)$
WZr and In/WZr	Bridging nitrate	1631–1625 1245–1210	ν(N═O) $\nu_{as}(NO_2)$
	Bidentate nitrate	1579–1560 1245–1210	ν(N═O) $\nu_{as}(NO_2)$
	Monodentate nitrate	1537 1282–1268	$\nu_{as}(NO_2)$ $\nu_s(NO_2)$
	NO^+	2130	ν(NO)

The integrated areas of the peaks of nitrate species in the range of 1700–1400 cm^{-1} in Fig. 5(a) and (c) are displayed as a function of temperature in Fig. 6. The amount of nitrate adsorbed on WZr was much less than that adsorbed on In/ZrO_2, and the obvious decrease in nitrate adsorbed on former catalysts began at a lower temperature of 400 °C, while in the latter case, it occurred at 350 °C. This result indicates that the nitrate species adsorbed on WZr is more unstable than that on In/ZrO_2: the strong acid of WZr (one solid superacid) may reduce the alkaline sites and the intensity for NO_x adsorption. Due to the existence of InO^+, a promoter to decompose nitrate, the amount of NO_x ad species on In/WZr was less than that on WZr.

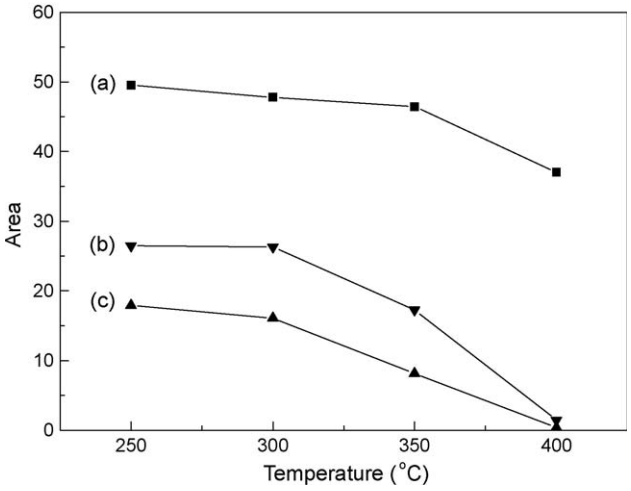

Fig. 6. Temperature dependence of the integrated areas of the peak of nitrate over In/ZrO_2 (a), WZr (b) and In/WZr (c) in the range of 1700–1400 cm^{-1}.

3.3.2. Surface species formed from CH_4 activation

Upon heating the catalyst of In/ZrO_2 to 250 °C in a gas flow of 0.3% CH_4 (N_2 as balance), some weak bands appeared in the range of 1700–1400 cm^{-1} (Fig. 7(a)). The bands between 1594 and 1685 cm^{-1} stem from the adsorbed H_2O vibration, while the bands at 1536, 1454 and 1413 cm^{-1} can be attributed to carbonate species: bidentate carbonate at 1536 cm^{-1}; monodentate carbonate at 1454 and 1413 cm^{-1}. At 350 °C, the peak of H_2O vibration disappeared while that of carbonate species gained strength in intensity. The results indicated that the complete oxidation of CH_4 occurring on In/ZrO_2 in the absence of O_2 may be caused by the active oxygen atom on the surface of the catalyst.

Three obvious bands, centered at 1610, 1566 and 1540 cm^{-1}, developed when CH_4/N_2 was flowed over WZr catalyst at 250 °C (Fig. 7(b)). The strongest band at 1610 cm^{-1} was attributed to H_2O vibration, while the band at 1540 cm^{-1} was assigned to bidentate carbonate, which was also detected on the In/ZrO_2 catalyst. As a result of the strong acidity of WZr, which has a large adsorption capacity for bipolarity molecular of H_2O, the band intensity of H_2O vibration was much larger than that adsorbed on In/ZrO_2. However, for the adsorbed carbonate intensity, stemmed from the acidity of gaseous CO_2, is just the opposite. In Kantcheva and Vakkasoglu's study [30], the band at 1566 cm^{-1} is assigned to $HCOO^-$. Usually, an accompanied peak at 1650 cm^{-1} belonging to $HCOO^-$ emerges simultaneously. However, no obvious peaks are observed at 1650 cm^{-1}, we speculate that this peak might be covered by the H_2O peak. Upon increasing temperature to 350 °C, the band of H_2O became weaker, and as expected, brought out the peak of $HCOO^-$. The results suggest that CH_4 was partially oxidized on WZr rather than fully oxidized to H_2O and CO_2 as on In/ZrO_2.

Fig. 7(c) shows the IR bands of the CH_4 activation species on In/WZr under the applied reaction conditions. At 250 °C, vibration at 1610 cm^{-1}, stemming from H_2O, is still the strongest band, while a weak peak is observed at about 1550 cm^{-1}. Moreover, the latter gains intensity at 1554 cm^{-1} when the temperature climbed to 350 °C. Because of the weak adsorption of carbonate on the carrier of superacid, it is difficult to attribute such strong vibration bands to carbonate species. The band of bidentate carbonate in previous studies is no more than 1550 cm^{-1}, while $HCOO^-$ peaks always emerge at 1560–1550 cm^{-1} [30,32,42]. Therefore, the assignment of this strong band to the $HCOO^-$ species would be more reasonable. In addition, the shift from 1566 cm^{-1} (over WZr) to 1554 cm^{-1} (over In/WZr) might be associated with the presence of indium in In/WZr catalyst.

Table 2 summarizes the peak assignment of the CH_4 activation species on In/ZrO_2, WZr and In/WZr based catalysts.

3.3.3. Surface species formed from the reaction between adsorbed NO_x species and CH_4

Fig. 8(a) shows the interaction of CH_4 with the catalyst of WZr containing adsorbed NO_x species at various temperatures. After

Table 2
Assignment of the IR bands in CH_4 activation experiments.

Catalyst	Species	Wave numbers (cm^{-1})	Vibration
In/ZrO_2	H_2O	1594–1685	$\delta(H_2O)$
	Bidentate carbonate	1540–1536	ν(C═O)
	Monodentate carbonate	1454, 1413	$\nu_{as}(CO_2)$, ν_s(CO)
WZr and In/WZr	H_2O	1614–1610	$\delta(H_2O)$
	Bidentate carbonate	1540–1538	ν(C═O)
	$HCOO^-$	1660–1658	ν(C═O)
		1566–1554	$\nu_{as}(CO_2)$

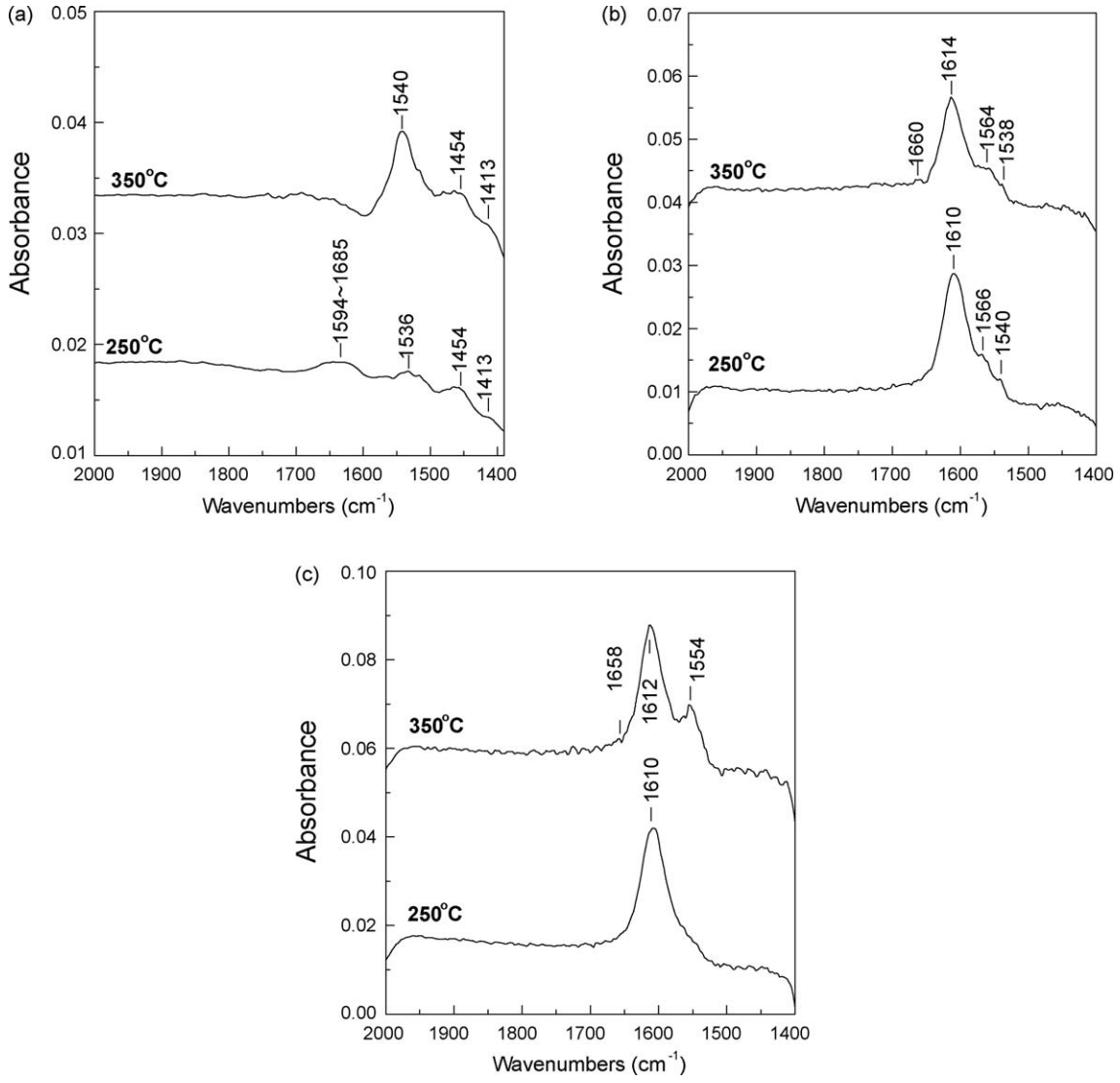

Fig. 7. In situ DRIFT spectra of CH_4 activation species over In/ZrO_2 (a), WZr (b) and In/WZr (c) at 250 and 350 °C.

adsorption with 0.1% NO + 10% O_2 at room temperature and purging with 20 mL/min N_2 at 250 °C, stable nitrate species were formed on the surface of catalyst. The attribution of the species is the same as shown in Table 1. Although these species decomposed gradually with increasing temperature, they hardly changed with the addition of 0.3% CH_4 to the gas flow at 250 °C. Within the temperature range of 250–350 °C, the change of the nitrate species is similar with that observed in NO_x adsorption–desorption experiment, as described in Section 3.3.1. This suggests that these stable nitrate species were unable to activate CH_4 directly. At 400 °C, the nitrate species disappeared and a series of new bands developed from CH_4 activation, which are attributed to H_2O (at 1615 cm^{-1}), $HCOO^-$ (at 1565 cm^{-1}) and carbonate (at 1546, 1448, and 1413 cm^{-1}) (magnified in Fig. 8(b)).

Similar surface species were formed on the catalyst of In/WZr as that on WZr after adsorption of NO_x at room temperature and desorption in N_2 at 250 °C (Fig. 9(a)). Upon adding 0.3% CH_4 to the gas flow, the species remained unchanged at that temperature. After raising the temperature to 300 °C, a slight decomposition of nitrate species was observed, but without the development of a new species. However, once the temperature reached 350 °C, the band at 1211 cm^{-1} became very weak, and the bands at 1628 and 1573 cm^{-1} shifted to 1621 and 1558 cm^{-1}, respectively (Fig. 9(b)). The results demonstrate that nitrate species was decomposed; meanwhile, H_2O and $HCOO^-$ were formed during temperature raising process. H_2O, $HCOO^-$ and carbonate became the main surface species associated with the disappearance of the nitrate species as the temperature rose to 400 °C.

3.3.4. Steady-state in situ DRIFTS study of CH_4-SCR of NO over WZr and In/WZr

Two strong infrared bands developed in the 1700–1500 cm^{-1} frequency region (at 1628 and 1602 cm^{-1}) when $NO/CH_4/O_2$ were flowed over the WZr catalyst at the temperatures from 300 to 450 °C (Fig. 10). These bands differ from the bands that originated from the nitrate species formed in NO_x adsorption–desorption experiments (Fig. 5(b)), as well as the CH_4 activation species formed in CH_4 activation experiment (Fig. 7(b)). In a stable reaction process where the species of nitrate is adsorbed on the surface of the catalyst, the presence of NO_2 in the gas flow will also give rise to absorption bands at that frequency region [32,43]. Thus, the bands at 1628 and 1602 cm^{-1} might be the overlap peaks of NO_2 and surface nitrate species. The band at 1211 cm^{-1} is attributed to the nitrate species, which will be completely decomposed at 400 °C. This result is in accordance with the results of the NO_x adsorption–desorption experiment and the NO_x-CH_4 reaction experiment described above. At 450 °C, all the nitrate species decomposed and the bands at 1628 and 1602 cm^{-1} were generated only from NO_2 in the gas phase.

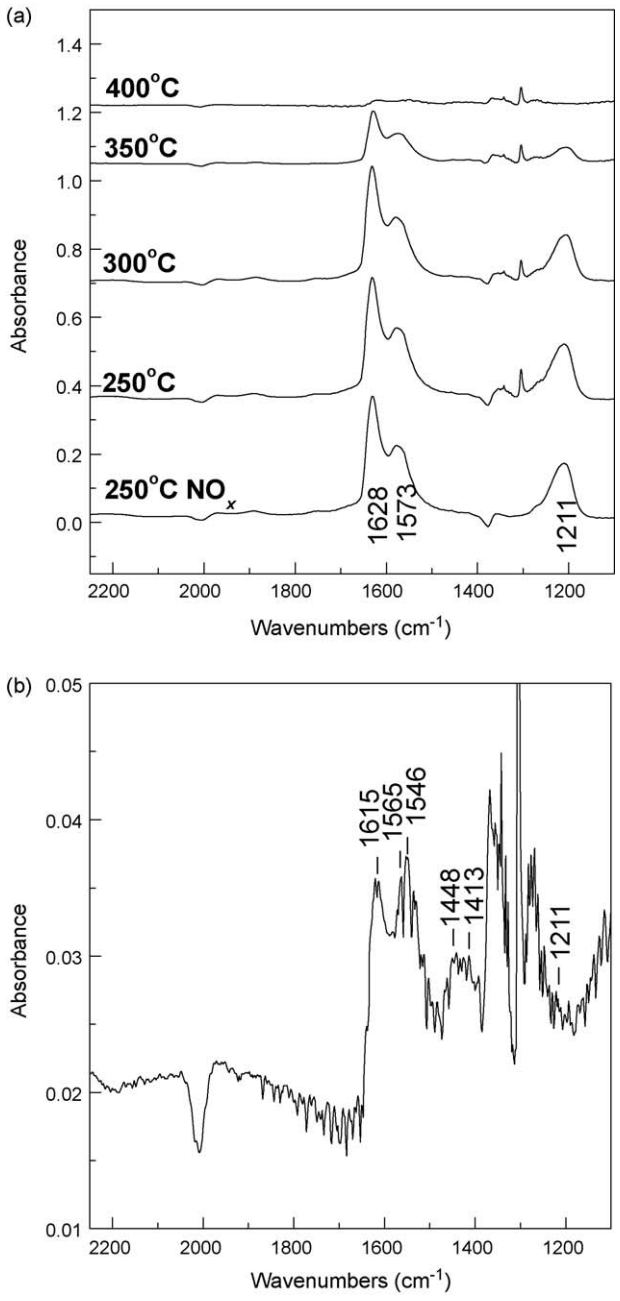

Fig. 8. In situ DRIFT spectra of surface species formed from the reaction between adsorbed NO_x species and CH_4 over WZr catalyst: (a) at 250, 300, 350 and 400 °C; (b) magnified of 350 and 400 °C.

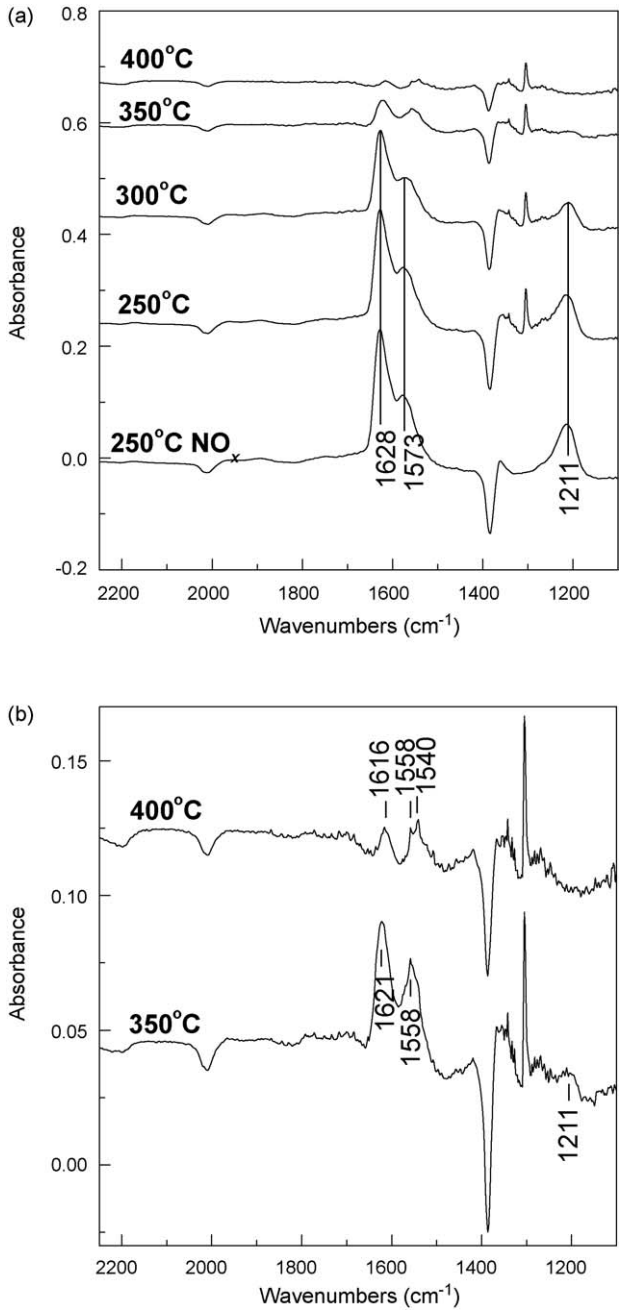

Fig. 9. In situ DRIFT spectra of surface species formed from the reaction between adsorbed NO_x species and CH_4 over In/WZr catalyst: (a) at 250, 300, 350 and 400 °C; (b) magnified of 350 and 400 °C.

It is necessary to point out that the activation species of CH_4 (H_2O, $HCOO^-$ and carbonate), whose bands might be covered by the strong bands of nitrate and NO_x, failed to be detected in this test.

Using the In/WZr catalyst in the experiment, the bands developed at 300 °C are similar to that on the WZr carrier, located at 1628, 1602 and 1211 cm^{-1}, respectively (Fig. 11(a)). As the temperature rose to 350 °C, in contrast to the spectra obtained from WZr catalyst, the nitrate species, giving rise to the bands at 1628, 1602 and 1211 cm^{-1}, were decomposed completely. Simultaneously, the double peaks located in the 1700–1500 cm^{-1} frequency range converted to a single peak, centered at 1610 cm^{-1}, suggesting the formation of H_2O. In addition, the peaks of NO_2 might be covered by the strong vibration of H_2O. Also, a new weak band, attributed to $HCOO^-$, developed at 1552 cm^{-1}. This observation is in agreement with the result of the NO_x-CH_4 reaction experiment, supporting the relationship between the appearance of the new surface species and CH_4 activation. Increasing temperature from 350 to 500 °C, as expected, resulted in the weakening of the peak at 1610 cm^{-1} and the rising and subsequent declining of the peak at 1552 cm^{-1}. The integrated areas of peaks of $HCOO^-$ in Fig. 11(a) are displayed as a function of temperature in Fig. 11(b). The amount of $HCOO^-$ appears maximized at 450 °C, in accordance with NO_x conversion results shown in Fig. 1(a). According to these results, the surface $HCOO^-$ species is substantiated as a key intermediate of the CH_4-SCR of NO_x.

3.3.5. Transient response of the CH_4-SCR reaction on In/WZr

Fig. 12(a) shows the real-time change of the IR spectra over the In/WZr catalyst after the sudden addition of NO to the gas flow of the $CH_4 + O_2$ mixture. Before the onset of the SCR reaction over the In/WZr catalyst, similar bands developed at 1610 and 1552 cm^{-1},

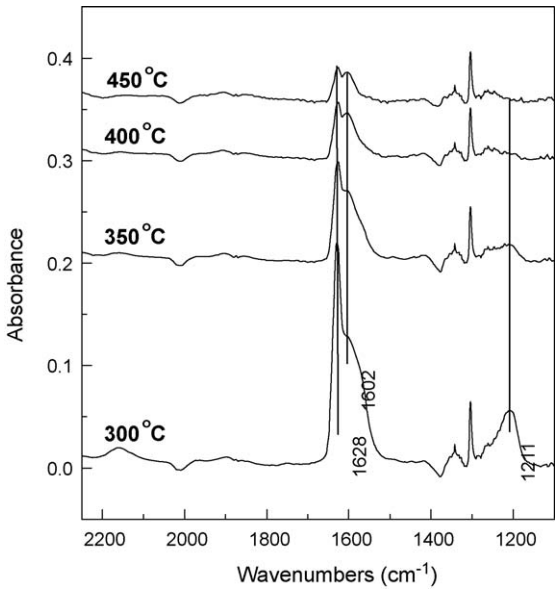

Fig. 10. In situ DRIFT spectra of surface species formed from steady-state CH_4-SCR over WZr catalyst at various temperatures (from 300 to 450 °C).

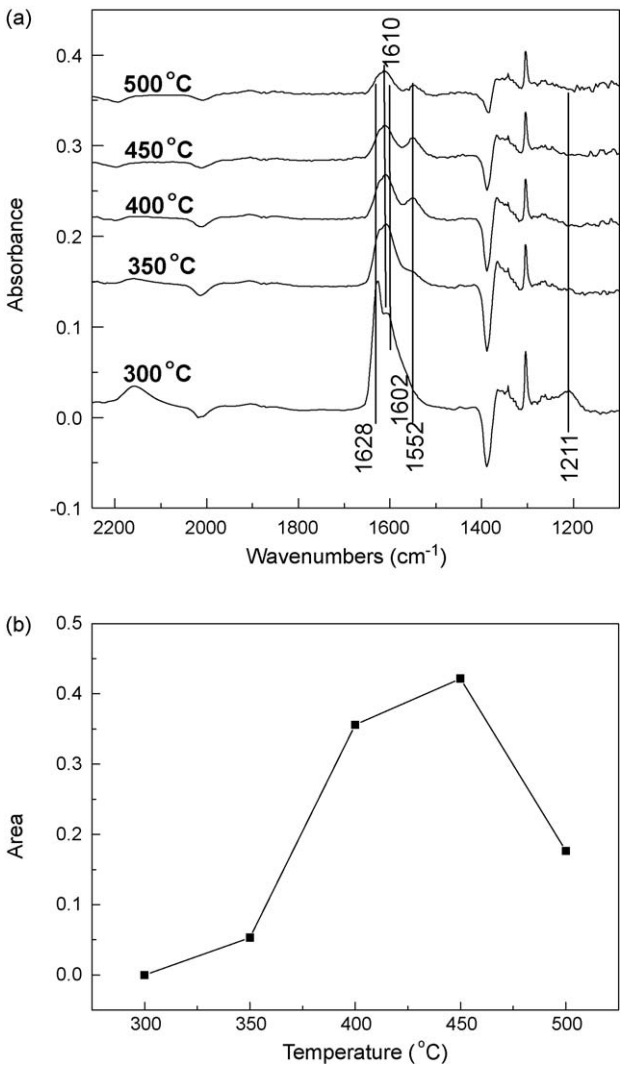

Fig. 11. (a) In situ DRIFT spectra of surface species formed from steady-state CH_4-SCR over In/WZr catalyst at various temperatures (from 300 to 450 °C). (b) Temperature dependence of the integrated areas of the peak of $HCOO^-$ over In/WZr in the range of 1580–1480 cm^{-1}.

assigned to H_2O and $HCOO^-$ respectively, in the CH_4/O_2 flow for 20 min at 400 °C. The addition of NO to the reaction mixture resulted in a quick formation of a shoulder peak of NO_2 at 1628 cm^{-1}, while the former two bands gained intensity gradually, suggesting that the adsorption species from NO promoted the activation of CH_4 as depicted in Section 3.3.3. The IR bands of nitrate specie at 1211 cm^{-1} were undetected due to its easy decomposition at 400 °C. However, the fast reaction between $HCOO^-$ and those active nitrate species might bring out the formation of N_2. To compare these two species, the amount of $HCOO^-$ was larger than that of active nitrate. We speculate that the formation of the nitrate species from NO governs the rate of NO_x conversion. This process includes two steps: the oxidation of NO to NO_2 and the adsorption of NO_2 to form nitrate species over catalyst. On the sudden removal of CH_4 from the reaction mixture, as shown in Fig. 12(b), the bands of NO_2 (at 1628 and 1602 cm^{-1}) gained in intensity as time continued, while the band of $HCOO^-$ decreased quickly and disappeared after 5 min, indicating that $HCOO^-$ was very active in reaction with the surface nitrate species.

Upon reversing the process of Fig. 12(a), as expected, the bands of NO_2 (at 1628 and 1602 cm^{-1}) weakened in intensity, while the band of $HCOO^-$ and H_2O strengthened when CH_4 was added to the gas flow after equilibrium adsorption in NO + O_2 mixture over In/WZr (Fig. 12(c)). Accordingly, on the sudden removal of NO from the reaction mixture, as shown in Fig. 12(d), the shoulder peaks of NO_2 disappeared quickly, and the bands of H_2O (at 1610 cm^{-1}) and $HCOO^-$ (at 1552 cm^{-1}) weakened gradually until stable surface species formed after 20 min.

4. Discussions

4.1. Active indium species

As detected by XPS in our previous study [18], the active indium species on tungstated samples were InO^+, while on In/ZrO_2, the In_2O_3 bulk phase was the main species of indium. Many authors [5–7,19–21] have reported that the InO^+ specie is responsible for the conversion of NO on the indium supported zeolite catalyst, although the In_2O_3 bulk phase was not active for either the reduction of NO_x or the combustion of CH_4. On the In/WZr catalyst, the InO^+ species, as discussed above, was attributed to the active site for NO_x reduction. WZr might play the same role with ZSM-5, providing strong acid site for the anchoring of InO^+ species [23]. In addition, the entire CH_4 conversion curve of In/WZr shifted toward a much lower temperature than that of WZr, suggesting that the InO^+ species was not only responsible for NO_x reduction, but was also an active site for CH_4 oxidation. On ZrO_2, oxygen species served as the active center, which was similar to that of metal oxides catalysts such as La_2O_3 and Y_2O_3 [44]. The loading of indium on ZrO_2 cannot form the InO^+ species due to the lack of Brønsted acid sites. On the contrary, the covered In_2O_3 bulk phase decreased the surface areas and pore volumes, which were 27 m^2/g and 0.13 cm^3/g for ZrO_2, and 24 m^2/g and 0.12 cm^3/g for In/ZrO_2, respectively [18]. Consequently, NO_x conversion decreased.

4.2. The formation of $HCOO^-$ species

The DRIFTS analysis showed that $HCOO^-$ was the activation species on WZr and In/WZr catalysts. These findings differ from those observed on SZr. According to previous report [30], $HCOO^-$ was generated on the catalyst of Co/SZr instead of SZr during CH_4 activation. Supported by many literatures [45,46], hydrocarbons can be decomposed to an HC radical on a superacid surface. Li and

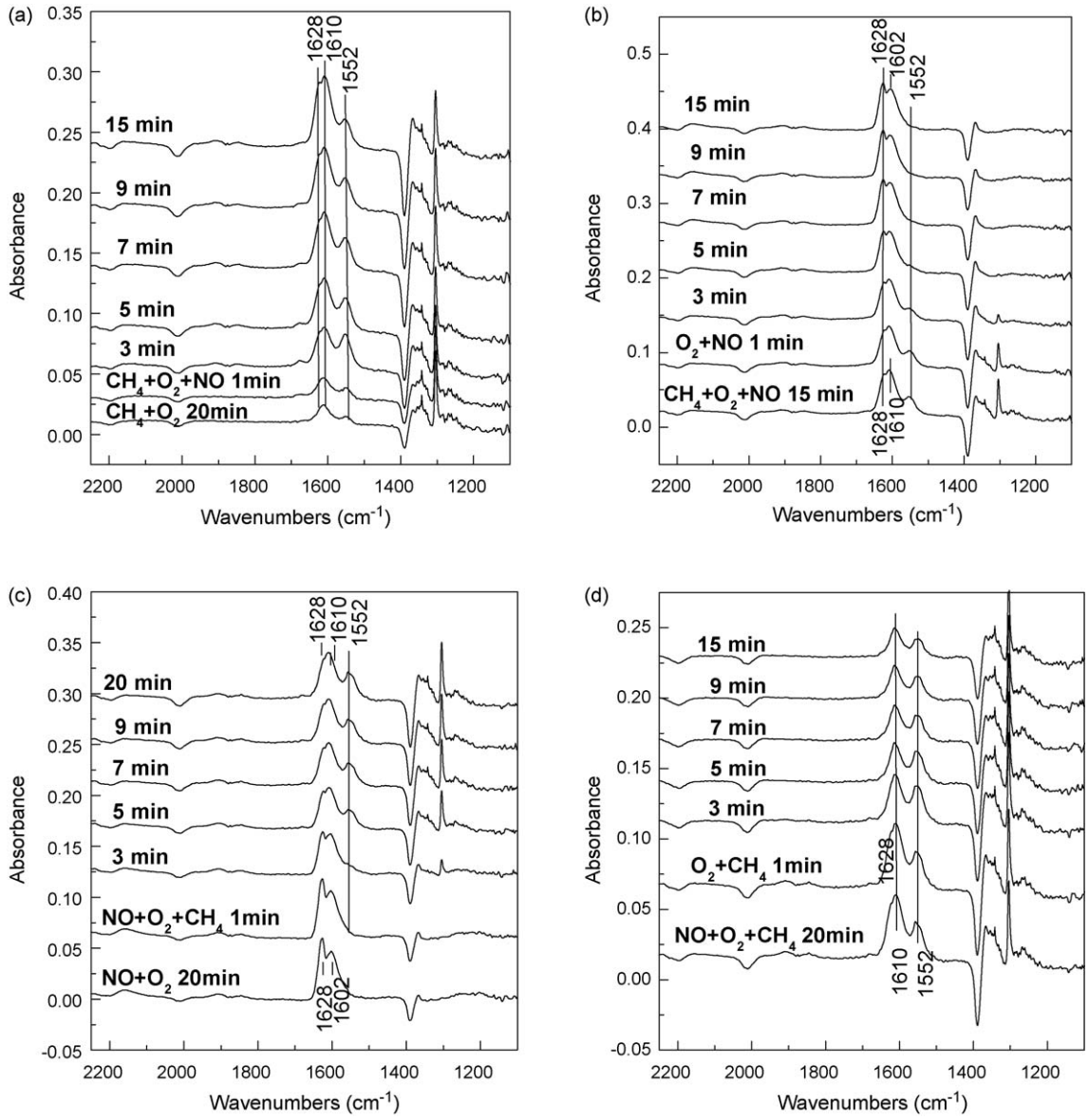

Fig. 12. In situ DRIFT spectra of surface species formed from transient CH_4-SCR over In/WZr catalyst at 400 °C. (a) Changes of surface species after addition of NO in $CH_4 + O_2$ mixture. (b) Changes of surface species after removal CH_4 from gas mixture of $CH_4 + NO + O_2$. (c) Changes of surface species after addition of CH_4 in $NO + O_2$ mixture. (d) Changes of surface species after removal NO from gas mixture of $CH_4 + NO + O_2$.

Armor [2] also deduced the conversion of CH_4 to $CH_3^\bullet$ by NO_2 adsorption on Co^{2+} site. Therefore, $CH_3^\bullet$ might be the first intermediate in CH_4 activation on a superacid catalyst and some zeolite-based catalysts. If there exists an active oxygen atom (O*), it can react with $CH_3^\bullet$ to form CH_3O^-, and further oxidized to $HCOO^-$. On the catalyst of SZr, CH_4 could decompose, but produce no $HCOO^-$ species due to the absent of O* supply. On the catalyst of Co/SZr, cobalt oxide provides O* to convert the intermediate specie of $CH_3^\bullet$ to $HCOO^-$. Kantcheva and Vakkasoglu [30] suggest the formation of $HCOO^-$ through Eqs. (1)–(3); the reaction of $HCOO^-$ and NO_3^- or NO_2 brings out the final products of N_2 and CO_2 (Eq. (4)):

$$CH_4 + Co^{2+}{-}O^{2-} \rightarrow [CH_3{-}Co]^+ + OH^- \quad (1)$$

$$[CH_3{-}Co]^+ + O^{2-} \rightarrow CH_3{-}O^- + Co^0 \quad (2)$$

$$CH_3O^- + 2(Co^{2+}{-}O^{2-}) \rightarrow HCOOH + OH^- + 2Co^0 \quad (3)$$

$$HCOOH(HCOO^-) \xrightarrow{NO_3^-(NO_2)} CO_x, H_2O, N_2 \quad (4)$$

Differing from SZr, on the surface of WZr the conversion of CH_4 to $HCOO^-$ complete successfully because of the supplication of O* by WO_3. From the above speculation, the formation of $HCOO^-$ on WZr is deduced as follows (Eqs. (5)–(8)):

$$CH_4 \rightarrow CH_3^\bullet + H^\bullet \quad (5)$$

$$WO_3 \rightarrow WO_2 + O* \quad (6)$$

$$CH_3^\bullet + O* \rightarrow CH_3O^- \quad (7)$$

$$CH_3O^- + 2O* \rightarrow HCOO^- + H_2O \quad (8)$$

On In/WZr, by comparing the band intensity at 350 °C in Figs. 7(c) and 9(b), we found that the mount of $HCOO^-$ produced in the NO_x-CH_4 reaction experiment is triple of that produced in the CH_4 activation process, indicating that nitrate species enhanced the formation of $HCOO^-$. However, the promotion effect of the nitrate adspecies on WZr is unapparent (Fig. 8); therefore, we speculate that the nitrate species adsorbed on InO^+ site accelerates the formation of $HCOO^-$. However, the nitrate species was unable to

directly react with CH_4 to form $HCOO^-$ because very little $HCOO^-$ formed at a temperature below 300 °C. It is important to note that the promotion effect of nitrate species to $HCOO^-$ formation emerged at 350 °C (Fig. 5(c)). At that temperature, most of the nitrate species covering WZr had been decomposed and the active sites on the surface of WZr were exposed to CH_4, spurring the conversion of CH_4 to $CH_3^\bullet$ (Eq. (1)). The role of the nitrate adsorbing on InO^+ was to offer active oxygen for further $CH_3^\bullet$ oxidation, making the CH_4 activation smoother (Eqs. (7)–(9)).

$$[InO^+(NO_2)]_{ads} \rightarrow InO^+ + NO + O* \quad (9)$$

Beltramone [47] supports the conclusion that the activation of methane is initiated by NO_2 and NO_3^- hemisorbed species on InO^+ sites of the In-ZSM-5 zeolite.

4.3. Reaction mechanism

The experimental results show that the formation of $HCOO^-$ on the catalyst surface can be easy detected, not only over the In/WZr catalyst, but also over the WZr carrier, which is in agreement with the results of Kantcheva and Cayirtepe [32]. The adsorbed nitrate species and the HCOO– are substantiated as key intermediates of the CH_4/NO-SCR reaction in the presence of O_2. In view of these findings, we propose a simplified reaction scheme for the NO_x reduction by CH_4 on In/WZr (Fig. 13). Due to the impossibility of NO adsorbing directly on catalyst surface to form nitrate species, the oxidation of NO to NO_2 is the only way to form nitrate species. The oxidation of NO to NO_2 is now generally accepted to be an important reaction step to improve NO_x reduction by CH_4 [48–50]. It was confirmed by the observation of NO_2 in the stable and transient experiment described above and the promotion effect of NO_2 on the CH_4-SCR process, as shown in Fig. 2. On In/WZr catalyst, nitrate species formed from the adsorbed NO_2, were adsorbed on two different sites. One was adsorbed on the WZr carrier and the other was adsorbed on the InO^+ site. At low temperatures, active sites for CH_4 activation were covered by nitrate species, which impeded the CH_4-SCR reaction. Maunula et al. [6] have revealed the existence of inhibiting compounds like nitrates and carbonates at lower temperatures on In/ZSM-5. They observed that low coverage on the catalysts' surface gave the highest NO conversion under their reduction conditions. Therefore, upon increasing temperature, nitrate species adsorbed on the WZr carrier disappear and the active sites are restored to maintain the CH_4 activation and SCR reaction at 350 °C. The formation of $HCOO^-$, one key intermediate for CH_4-SCR, is attributed to the uncovered WZr carrier and the NO_3^- species adsorbed on the InO^+ site. The WZr carrier induces CH_4 decomposition and the NO_3^- species adsorbed on InO^+ provides active oxygen (Eqs. (5) and (7)–(9)). The formation of N_2 involves the interaction between the intermediates of $HCOO^-$ and nitrate species, in agreement with Kantcheva's study on Pd/WO_3-ZrO_2 [32,43] and Co/SZr [30].

4.4. Effect of tungstation

Tungstation affects the properties of support in several aspects. Firstly, tungstation of ZrO_2 changes the acidity of the support,

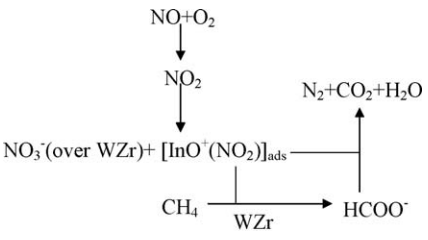

Fig. 13. The possible mechanism of the SCR of NO_x by CH_4 over In/WZr catalyst.

which is responsible for the formation of the active indium species, namely InO^+, on In-loaded tungstated zirconia. The experimental results of Kikuchi et al. [5] suggest that the formation of InO^+ takes place between In_2O_3 and the Brønsted acid sites on zeolite. The reaction is as follows:

$$In_2O_3 + 2H^+ - Z^- \rightarrow 2InO^+ - Z^- + H_2O$$

In this work, strong Brønsted acid sites are detected on the surface of tungstated catalysts by Py-IR analysis (see Fig. 3), which induces the formation of InO^+. XPS results also confirm the existence of InO^+ on the surface of In/WZr. On the other hand, all acid sites on ZrO_2 were Lewis sites. Naturally, the state of indium on In/ZrO_2 was the In_2O_3 bulk phase due to the lack of Brønsted acid sites. Secondly, tungstation weakens the oxidative ability and deters the further oxidation of methane, which brings out the key intermediate of $HCOO^-$ in NO_x conversion to N_2. While on In/ZrO_2 and ZrO_2, the activation product of methane was CO_2 and H_2O. Thirdly, the combination of InO^+ and tungstation accelerates the formation of $HCOO^-$ and the reduction of nitrate species. On ZrO_2 and In/ZrO_2, even at 400 °C, there is still a large amount of adsorbed nitrate species. After tungstation, the adsorption ability is weakened by the strong acidity and the adspecies are easily decomposed at lower temperature. The exposure of the active sites accelerates the SCR reaction. However, without InO^+, the amount of $HCOO^-$ is very small on WZr carrier, and even failed to be detected in the steady-state experiment (Fig. 9), while on In/WZr, the formation of $HCOO^-$ is accelerated greatly by the cooperation of InO^+ and tungstation. As a result, NO_x conversion efficiency is facilitated.

In a word, tungstation changed the mechanism of the reactions by influencing the reaction intermediates and the active sites of the catalyst. In this way, the cooperation of tungstation and the loading of indium result in the highest activity of In/WZr in comparison to WZr and In/ZrO_2.

5. Conclusion

Indium was present on the WZr carrier in two forms, InO^+ and In_2O_3. Only the former has catalytic activity in CH_4-SCR of NO. The effect of tungstation is to provide Brønsted acid sites, which lead to the formation of InO^+. In situ FTIR experiments at low temperatures reveal the existence of inhibiting compounds like the nitrate species for CH_4 activation. On ZrO_2 and In/ZrO_2 catalysts, observations show the difficulty of CH_4 activation to form surface species of $HCOO^-$ due to the surface coverage of abundant nitrate species at temperatures below 400 °C. Moreover, the activation species of CH_4 on these catalysts are H_2O and CO_2, rather than oxygenic organics available to NO_x reduction. Both of the previous ways determine the low activity of CH_4-SCR of NO over ZrO_2 and In/ZrO_2 catalysts. However, because of the strong acid of WZr, the adsorption of nitrate species is weakened and easy to be decomposed at low temperature. Except for H_2O and CO_2, the adsorbed $HCOO^-$ intermediate, proposed to be the actual NO reductant in the mechanism of CH_4-SCR is detected in a small amount in the experiment of CH_4 activation on WZr. The formation of $HCOO^-$ is increased greatly by the cooperation of tungstation and InO^+; furthermore, the surface coverage of nitrate species under the reduction conditions was very low, accordingly, giving the highest NO conversion on In/WZr catalyst.

Acknowledgements

This work was financially supported by the National Natural Science Fund of China (Grant No. 20677034) and the National High-Tech Research and Development (863) Program of China (Grant Nos. 2006AA060301 and 2006AA06A304).

References

[1] Y. Li, J.N. Armor, Appl. Catal. B 1 (1992) 31–40.
[2] Y. Li, J.N. Armor, Catal. Today 26 (1995) 147–158.
[3] X.J. Zhou, T. Zhang, Z.S. Xu, L.W. Lin, Catal. Lett. 40 (1996) 35–38.
[4] X.J. Zhou, Z.S. Xu, T. Zhang, L.W. Lin, J. Mol. Catal. A 122 (1997) 125–129.
[5] E. Kikuchi, M. Ogura, I. Terasaki, Y. Goto, J. Catal. 161 (1996) 465–470.
[6] T. Maunula, J. Ahola, H. Hamada, Appl. Catal. B 64 (2006) 13–24.
[7] E.E. Miro, L. Gutierrez, J.M. Ramallo Lopez, F.G. Requejo, J. Catal. 188 (1999) 375–384.
[8] T. Sowade, T. Liese, C. Schmidt, F.W. Schutze, X. Yu, H. Berndt, W. Grunert, J. Catal. 225 (2004) 105–115.
[9] T. Maunula, J. Ahola, H. Hamada, Ind. Eng. Chem. Res. 46 (2007) 2715–2725.
[10] A. Kubacka, J. Janas, B. Sulikowski, Appl. Catal. B 69 (2006) 43–48.
[11] O.A. Anunziata, A.R. Beltramone, F.G. Requejo, J. Mol. Catal. A: Chem. 267 (2007) 194–201.
[12] O.A. Anunziata, A.R. Beltramone, E.J. Lede, F.G. Requejo, J. Mol. Catal. A: Chem. 267 (2007) 272–279.
[13] W. Suprun, K. Schaedlich, H. Papp, Chem. Eng. Technol. 28 (2005) 199–203.
[14] C.J. Looughran, D.E. Resasco, Appl. Catal. B 7 (1995) 113–126.
[15] Y.H. Chin, W.E. Alvarez, D.E. Resasco, Catal. Today 62 (2000) 291–302.
[16] A. Ali, Y.H. Chin, D.E. Resasco, Catal. Lett. 56 (1998) 111–117.
[17] A.W. Aylor, L.J. Lobree, J.A. Reimer, A.T. Bell, J. Catal. 172 (1997) 453–462.
[18] D. Yang, J.H. Li, M.F. Wen, C.L. Song, Catal. Commun. 8 (2007) 2243–2247.
[19] X. Zhou, Z. Xu, T. Zhang, L.W. Lin, J. Mol. Catal. A 122 (1997) 125–129.
[20] O.A. Anunziata, A.R. Beltramone, E.J. Lede, F.G. Requejo, J. Mol. Catal. A 267 (2007) 272–279.
[21] O.A. Anunziata, A.R. Beltramone, F.G. Requejo, J. Mol. Catal. A 267 (2007) 194–201.
[22] E. Kikuchi, M. Ogura, Catal. Surv. Jpn. 1 (1997) 227–237.
[23] L.B. Gutierrez, J.M. Ramallo-Lopez, S. Irusta, E.E. Miro, F.G. Requejo, J. Phys. Chem. B 105 (2001) 9514–9523.
[24] F. Lonyi, J. Valyon, L. Gutierrez, M.A. Ulla, E.A. Lombardo, Appl. Catal. B 73 (2007) 1–10.
[25] A.D. Cowan, N.W. Cant, B.S. Haynes, P.F. Nelson, J. Catal. 176 (1998) 329–343.
[26] A. Satsuma, A.D. Cowan, N.W. Cant, D.L. Trimm, J. Catal. 181 (1999) 165–169.
[27] K. Shimizu, F. Okada, Y. Nakamura, A. Satsuma, T. Hattori, J. Catal. 195 (2000) 151–160.
[28] T. Montanari, O. Marie, M. Daturi, G. Busca, Appl. Catal. B 71 (2007) 216–222.
[29] L.J. Lobree, A.W. Aylor, J.A. Reimer, A.T. Bell, J. Catal. 181 (1999) 189–204.
[30] M. Kantcheva, A.S. Vakkasoglu, J. Catal. 223 (2004) 364–371.
[31] M. Kantcheva, A.S. Vakkasoglu, J. Catal. 223 (2004) 352–363.
[32] M. Kantcheva, I. Cayirtepe, Catal. Lett. 115 (2007) 148–162.
[33] D. Yang, J.H. Li, M.F. Wen, C.L. Song, Catal. Lett. 117 (2007) 68–72.
[34] L.L. Ren, T. Zhang, J.W. Tang, Appl. Catal. B 41 (2003) 129–136.
[35] J.A. Lercher, C. Grundling, G. EderMirth, Catal. Today 27 (1996) 353–376.
[36] K.T. de Campos Roseno, A.S. Maria Baldanza, S. Martin, Catal. Lett. 124 (2008) 59–67.
[37] N. Li, A.Q. Wang, M.Y. Zheng, X.D. Wang, R.H. Cheng, T. Zhang, J. Catal. 225 (2004) 307–315.
[38] K. Hadjiivanov, V. Avreyska, D. Klissurski, T. Marinova, Langmuir 18 (2002) 1619–1625.
[39] B. Tsyntsarski, V. Avreyska, H. Kolev, T.S. Marinova, D. Klissurski, K. hadjiiibanov, J. Mol. Catal. A 193 (2003) 139–149.
[40] C.E. Quincoces, S. Guerrero, P. Araya, M.G. Gonzalez, Catal. Commun. 6 (2005) 75–80.
[41] F.B. Noronha, E.C. Fendley, R.R. Soares, W.E. Alvarez, D.E. Resasco, Chem. Eng. J. 82 (2001) 21–31.
[42] M. Kantcheva, M.U. Kucukkal, S. Suzer, J. Catal. 190 (2000) 144–156.
[43] M. Kantcheva, K. Cayirtepe, J. Mol. Catal. A 247 (2006) 88–98.
[44] A. Vannice, A.B. Walters, X. Zhang, J. Catal. 159 (1996) 119–126.
[45] I.V. Bobricheva, I.A. Stavitsky, V.K. Yermolaev, N.S. Kotsarenko, V.P. Shmachkova, D.I. Kochubey, Catal. Lett. 56 (1998) 23–27.
[46] S. Kuba, P.C. Heydorn, R.K. Grasselli, B.C. Gates, M. Che, H. Hnozinger, Phys. Chem. Chem. Phys. 3 (2001) 146–154.
[47] A.R. Beltramone, L.B. Pierella, F.G. Requejo, O.A. Anunziata, Catal. Lett. 91 (2003) 19–24.
[48] A.P. Ferreira, S. Capela, P. Da Costa, C. Henriques, M.F. Ribeiro, F. Ramo Ribeiro, Catal. Today 119 (2007) 156–165.
[49] M. Misono, Y. Hirao, C. Yokoyama, Catal. Today 38 (1997) 157–162.
[50] H. Kato, C. Yokoyama, M. Misono, Catal. Lett. 47 (1997) 189–191.